Available online at www.sciencedirect.com
ScienceDirect
Carbon 44 (2006) 2516–2522
CARBON
www.elsevier.com/locate/carbon

Development of carbon nanotube and carbon xerogel supported catalysts for the electro-oxidation of methanol in fuel cells

J.L. Figueiredo [a,*], M.F.R. Pereira [a], P. Serp [b], P. Kalck [b], P.V. Samant [c], J.B. Fernandes [d]

[a] *Laboratório de Catálise e Materiais, Departamento de Engenharia Química, Faculdade de Engenharia, Universidade do Porto, 4200-465 Porto, Portugal*
[b] *Laboratoire de Catalyse, Chimie Fine et Polymères, Ecole Nationale Supérieure d'Ingénieurs en Arts Chimiques et Technologiques, 118 route de Narbonne, 31077 Toulouse Cedex 04, France*
[c] *Department of Chemistry, Government College of Arts Science and Commerce, Sanquelim, Goa 405 505, India*
[d] *Department of Chemistry, Goa University, Taleigao Plateau, Goa 403 206, India*

Received 31 October 2005; accepted 22 May 2006
Available online 7 July 2006

Abstract

Multiwalled carbon nanotubes and high surface area mesoporous carbon xerogel were prepared and used as supports for monometallic Pt and bimetallic Pt–Ru catalysts. In order to assess the influence of the oxygen surface groups of the support, the mesoporous carbon xerogel was also oxidized with diluted oxygen before impregnation. Various reduction protocols were tested, the best results corresponding to reduction with sodium borohydride. High dispersion catalysts were obtained, which showed quite good performance in the electro-oxidation of methanol. In particular, a remarkable increase in the activity was observed when the Pt–Ru catalysts were supported on the oxidised xerogel. This effect was explained in terms of the metal oxidation state, as shown by XPS. It has been shown that the oxidised support helps to maintain the metals in the metallic state, as required for the electro-oxidation of methanol. This effect was negligible in the case of the Pt catalysts.

Keywords: Carbon nanotubes; Carbon xerogels; Catalyst support; Oxidation; Electrochemical properties

1. Introduction

Direct methanol fuel cells (DMFCs) offer much promise as convenient and environmentally acceptable power sources for portable devices and electric vehicle applications. The electrochemical oxidation of methanol involves the following reactions:

$$CH_3OH + H_2O \rightarrow CO_2 + 6H^+ + 6e^- \quad \text{(anode)}$$

$$\frac{3}{2}O_2 + 6H^+ + 6e^- \rightarrow 3H_2O \quad \text{(cathode)}$$

However, due to the relatively poor methanol oxidation kinetics, there is a need for improved catalysts. Platinum based catalysts are used in the anode, as Pt is capable of activating the C–H bond cleavage in the temperature range of operation of DMFCs (25–130 °C). The mechanism of the reaction is believed to involve a series of dehydrogenation steps leading to the formation of adsorbed carbon containing intermediates such as $–CHO_{ads}$ and $–CO_{ads}$, which deactivate the Pt catalyst. Improved performance can be obtained by alloying with a less noble metal, such as Ru, which can form the adsorbed –OH species needed to oxidise the CO adsorbed on Pt by the bifunctional mechanism:

$$Ru + H_2O \rightarrow Ru - OH + H^+ + e^-$$

$$Ru - OH + Pt - CO \rightarrow Ru + Pt + CO_2 + H^+ + e^-$$

* Corresponding author. Tel.: +351 225081663; fax: +351 225081449.
E-mail address: jlfig@fe.up.pt (J.L. Figueiredo).

0008-6223/$ - see front matter © 2006 Elsevier Ltd. All rights reserved.
doi:10.1016/j.carbon.2006.05.033

Pt–Ru are currently the best anode catalysts for DMFCs. These catalysts are usually supported onto electrically conducting high surface area (>75 m^2/g) carbon blacks [1,2].

The nature of the support is most important, since it determines the dispersion and stability of the metal crystallites, the electronic properties of the metal, including metal-support interactions and the extent of alloying in bimetallic catalysts, mass transfer resistances and the ohmic resistance of the catalyst layer. Therefore, special attention has been given to alternative carbon materials as catalyst supports for DMFCs, including carbon nanofibers [3,4], carbon nanotubes [5–8], carbon nanocoils [9] and other structured carbons [10–12].

Carbon aerogels and xerogels are mesoporous materials which offer interesting properties for catalysis [13,14]. We have recently reported on the use of carbon xerogels as supports for high dispersion Pt catalysts [15,16]. In particular, we have observed that Pt supported onto a carbon xerogel was more active for the electro-oxidation of methanol than the conventional Pt/Vulcan XC72 [16].

In the present communication we extend our previous studies and report on the effect of various experimental parameters on the electroactivity of Pt and Pt–Ru catalysts supported on novel carbon materials, including carbon nanotubes and carbon xerogels.

2. Experimental

2.1. Carbon supports synthesis

Multi-walled carbon nanotubes were prepared by chemical vapour deposition using ethylene with a Fe catalyst [17]. The nanotubes were then treated in 5 M HNO_3 for 3 h in a Soxhlet. This support is designated as NT. The carbon xerogel was synthesized by the conventional sol–gel approach using formaldehyde and resorcinol [18]; the wet gel was dried sub-critically and then carbonized under nitrogen atmosphere at 800 °C. This support is designated as CX. An activated material was prepared by gasification of CX to 18% burn-off, with 5% oxygen in nitrogen at 400 °C. This support is designated as CX18. The detailed synthesis procedures have been previously described [19].

2.2. Catalyst preparation

10 wt.% Pt was loaded either on NT, CX or CX18 by incipient wetness impregnation, wherein a calculated amount of hexachloroplatinic acid dissolved in a minimum amount of water was added dropwise under vacuum and ultrasonic mixing. The catalysts were then dried under vacuum and kept overnight in an oven for further drying. These catalysts are designated as 10PtNT, 10PtCX and 10PtCX18, respectively.

Pt–Ru (1:1) catalysts with 10% (total) metal load were prepared by sequential impregnation on the carbon supports. Thus, 5 wt.% Ru was initially impregnated from a $RuCl_3$ solution. The catalyst was then dried under vacuum and kept overnight in an oven. Subsequently, 5 wt.% Pt was added from a calculated amount of the hexachloroplatinic acid precursor. These catalysts were designated as 10PtRuNT, 10PtRuCX and 10PtRuCX18.

Table 1
Nomenclature of the prepared catalysts

Metal loading	Reduction procedure	Support	Sample
10 wt.% Pt	0.1 M sodium borohydride	CX	10PtCX-S
		CX18	10PtCX18-S
		NT	10PtNT-S
	0.1 M sodium formate	NT	10PtNT-F
	hydrogen (350 °C, 2 h)	NT	10PtNT-H_2
	0.1 M hydrazine hydrate	NT	10PtNT-H
5 wt.% Ru + 5 wt.% Pt	hydrogen (350 °C, 2 h)	NT	10PtRuNT-H_2
	0.1 M sodium borohydride	CX	10PtRuCX-S
		CX18	10PtRuCX18-S
	0.1 M hydrazine hydrate	CX	10PtRuCX-H
		CX18	10PtRuCX18-H
	0.1 M sodium formate	CX	10PtRuCX-F
		CX18	10PtRuCX18-F

Reduction of the metal precursors was achieved by four different protocols:

- In the liquid phase, by slow addition of either 0.1 M sodium formate, or 0.1 M hydrazine hydrate or 0.1 M sodium borohydride, at 60 °C. The catalysts were subsequently washed in hot water and then dried in an oven. The different protocols are indicated by a letter at the end of the catalyst designation code: F, H, or S, respectively.
- In the gas phase, under hydrogen flow at 350 °C for 2 h, indicated by H_2 at the end of the catalyst code.

The catalysts prepared are listed in Table 1.

2.3. Characterization of supports and catalysts

Nitrogen adsorption isotherms at liquid nitrogen temperature were obtained with a Coulter Omnisorp 100 CX sorptometer, and were subsequently analysed by the *t*-plot using the standard isotherm for carbon materials. Both the BET (S_{BET}) and mesopore (S_{meso}) surface areas were determined.

The nature and amounts of oxygen surface groups were determined by temperature programmed desorption (TPD) with mass spectrometric detection, as explained elsewhere [19,20]. Upon heating, the surface oxygen groups decompose, releasing CO_2 and CO at characteristic temperatures [20].

The catalysts were characterized by X-ray photoelectron spectroscopy (XPS) with a VG Scientific ESCALAB 200 A spectrometer using non-monochromatized Mg Kα radiation (1253.6 eV), and by transmission electron microscopy (TEM) with a Philips CM12 instrument (120 kV). Some samples were additionally characterized by X-ray diffraction with a SIEMENS D5000 diffractometer using Cu Kα

radiation. Measurements were performed in the θ–2θ mode at room temperature.

2.4. Electrocatalytic tests

For the catalyst layer preparation, a paste was made using a 5% Nafion solution and isopropyl alcohol, mixed with the catalyst powder under ultrasonic bath. The thick slurry obtained was then evenly spread over Toray carbon paper and dried in an oven at 110 °C. In this way, 2–3 layers of the catalyst slurry were applied one over the other and dried at 110 °C. The geometric surface area of the electrode was about 1 cm^2, containing 10 mg of the catalyst, which contained approximately 1 mg of metal.

The catalysts were tested in the electro-oxidation of methanol at 60 °C in a conventional three electrode assembly, using a mixture of 1 M methanol and 1 M H_2SO_4 as electrolyte. A saturated calomel electrode (SCE) was used as reference, and platinum foil as a counter electrode. From the corresponding polarization curves, the electrocatalytic activity of the catalysts was measured in terms of the current delivered at an overpotential of 0.6 V.

3. Results and discussion

3.1. Properties of the supports

The properties of the three supports used are summarized in Table 2. Multi-walled carbon nanotubes present the lowest surface area, absence of micropores, and the amount of surface groups is very small. The xerogel supports present much larger surface areas, which are mainly related with the presence of mesopores. In addition, these materials show a very large concentration of surface oxygen groups, especially the activated xerogel (CX18), which correspond mainly to carboxylic anhydrides, lactones, phenol/ether and carbonyl/quinone groups [19].

Table 2
Textural and surface properties of the carbon supports

Support	S_{BET} (m^2/g)	S_{meso} (m^2/g)	$CO + CO_2$ (μ mol g^{-1})
NT	175	175	85
CX	724	524	926
CX18	1084	672	8454

3.2. Properties of the catalysts

The metal particle sizes of the catalysts supported on different carbon materials were determined from TEM analysis. Micrographs were obtained at several magnifications. As an example, Fig. 1 shows high magnification TEM micrographs of the 10%Pt and 10%Pt–Ru catalysts supported on carbon nanotubes after H_2 reduction, and Fig. 2 shows the corresponding histograms of particle sizes. The mean particle size was determined from the histograms (at least 100 particles have been measured for each histogram), and the results are shown in Table 3.

Concerning the nanotube supported catalysts, several conclusions can be drawn from this table and from inspection of the micrographs:

(1) For the monometallic samples, the dispersion of Pt is bimodal, i.e., there are small particles anchored on the support (diameter $\leqslant$ 15 nm), and very large particles (generally around 100 nm). These larger particles are clearly observed in low magnification micrographs (not included). In the case of sample 10PtNT-S, and only in this case, the large particles consist of an aggregation of small particles; it seems that the $NaBH_4$ treatment in solution prevents the formation of large particles;
(2) Concerning the activation of platinum, the best results are obtained with $NaBH_4$ and sodium formate;

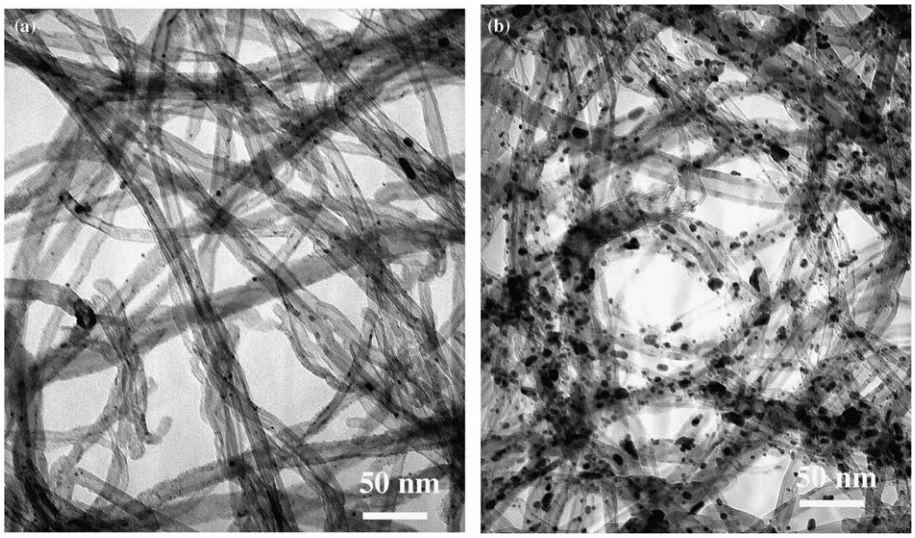

Fig. 1. TEM micrographs of NT-supported catalysts at high magnification. (a)10PtNT-H_2 and (b)10PtRuNT-H_2.

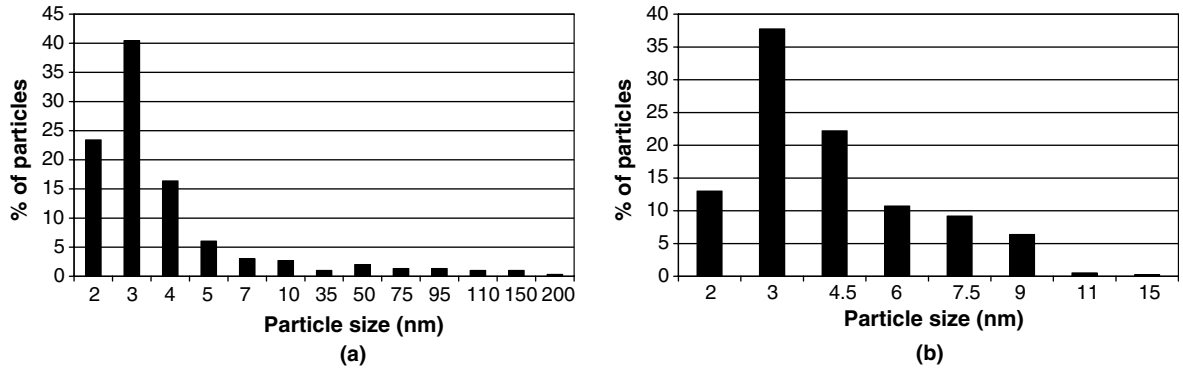

Fig. 2. Histograms of particle sizes obtained from TEM micrographs of NT-supported catalysts. (a)10PtNT-H_2 and (b)10PtRuNT-H_2.

Table 3
Particle sizes of the NT-supported catalysts, determined by TEM

Sample	Mean particle size (I)[a] (nm)	Mean particle size (II)[b](nm)
10PtNT-H_2	3.4	10
10PtRuNT-H_2	4.4	4.4
10PtNT-S	3.9	4.6
10PtNT-F	3.7	5.3

[a] Calculated from particles of mean size $\leqslant$15 nm.
[b] Calculated from all the particles.

(3) There is a pronounced effect of ruthenium pre-deposition on platinum dispersion. Indeed, for the bimetallic sample there is no bimodal particle size distribution, and only small particles are obtained. The bimetallic sample shows a very homogeneous metal deposition.

The average particle sizes obtained for the catalysts supported on the xerogels, CX and CX18, are included in Table 4. The Pt catalysts were reduced only with sodium borohydride (S), leading to monodispersed particle size distributions; the best dispersion was obtained on the oxidized support, CX18. Different reduction protocols were used in the case of PtRu catalysts. Relatively good dispersions were obtained on all samples, with the exception of 10PtRuCX18-F; possibly, this sample has not been properly reduced. In general, the samples show the presence of large agglomerates composed of smaller particles, with the exception of 10PtRuCX18-S, which shows no agglomerates. This sample is very homogeneous and well dispersed; only rare zones with large particles can be found.

X-ray diffraction patterns of the samples 10PtRuCX-S and 10PtRuCX18-S were recorded (data not shown). The diffraction peaks correspond to the characteristics lines of the fcc structure of Pt, but are slightly shifted to higher 2θ values. No lines are observed for ruthenium. These observations are indicative of Pt–Ru alloy formation, in agreement with many other reports [21–23]. Ruthenium can also be present as an amorphous $RuO_2 \cdot xH_2O$ phase, but this cannot be observed by XRD [21,23]. The width of the Pt(220) peak is not much different in both samples, in agreement with the results obtained by TEM.

3.3. Electrocatalytic activity

The results of the electrocatalytic tests at 60 °C are shown in Figs. 3–5, for the catalysts supported on NT, CX and CX18, respectively. The catalyst activities, expressed as the current delivered at an overpotential of 0.6 V (Amperes/gram of metal), are summarized in Table 5.

As expected, the Pt–Ru catalysts showed higher activities than the corresponding Pt catalysts.

Table 4
Particle sizes of the xerogel-supported catalysts, determined by TEM

Sample	Mean size (nm)	Observations
10PtCX-S	5.5	Range 2–15 nm
10PtCX18-S	3.5	Range 2–9 nm, very homogeneous
10PtRuCX-S	4–5	Big agglomerates of small particles
10PtRuCX-H	4.5	Agglomerates of small particles
10PtRuCX-F	4.0	Better dispersion, but large agglomerates
10PtRuCX18-S	5.0	Homogeneous and well dispersed; no agglomeration; rare zones with larger particles
10PtRuCX18-H	3–5	Many agglomerates of small particles
10PtRuCX18-F	5–50	A lot of large particles

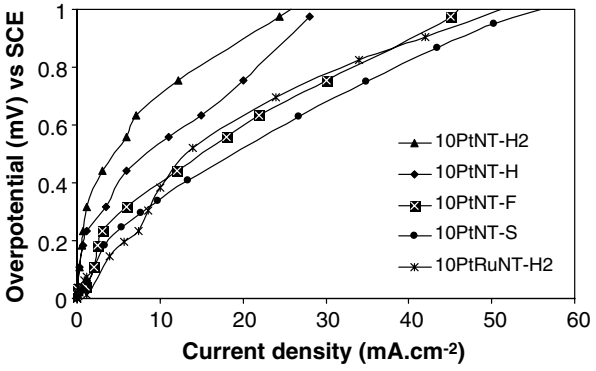

Fig. 3. Polarization curves for methanol oxidation at 60 °C. NT-supported catalysts.

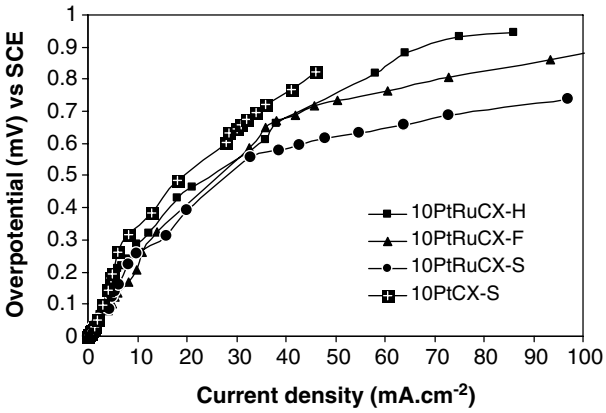

Fig. 4. Polarization curves for methanol oxidation at 60 °C. CX-supported catalysts.

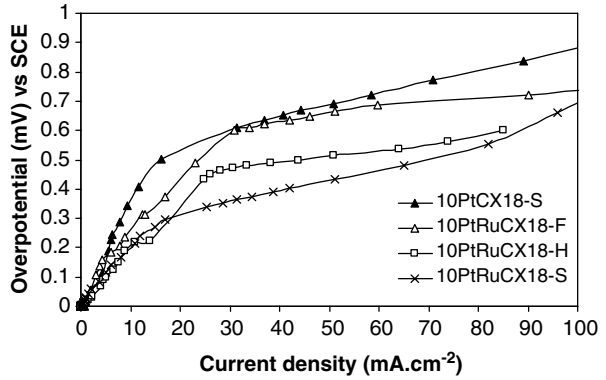

Fig. 5. Polarization curves for methanol oxidation at 60 °C. CX18-supported catalysts.

Table 5
Catalyst activities for electro-oxidation of methanol at 60 °C

Sample	Activity (A g^{-1})
10PtNT-H_2	6.1
10PtNT-H	13
10PtNT-F	20
10PtNT-S	25
10PtRuNT-H_2	17
10PtCX-S	28
10PtCX18-S	31
10PtRuCX-S	44
10PtRuCX-H	35
10PtRuCX-F	34
10PtRuCX18-S	85
10PtRuCX18-H	82
10PtRuCX18-F	32

Comparing the activities of the catalysts reduced by different procedures, it can be observed that the largest differences correspond to the NT-supported catalysts. Thus, 10PtNT-H_2 exhibits the lowest activity and the worst dispersion, while 10PtNT-S shows the best dispersion and highest activity. The differences are not so notorious in the case of the xerogel-supported catalysts, in correspondence with the good dispersions which were generally obtained (with the exception of 10PtRuCX18-F, as mentioned above). Nevertheless, the best results are also obtained with the samples reduced by sodium borohydride.

Taking sodium borohydride as the best reduction protocol, the results obtained with Pt catalysts supported on the three carbon materials can be compared. The electrocatalytic activities are found to increase in the order 10PtNT-S < 10PtCX-S < 10PtCX18-S. However, the effect of the support is not very important, as the activity increases of only about 10% from one support to another. In any case, the xerogel supports perform better than the nanotubes.

Considering now the performances of the Pt–Ru catalysts supported on the two xerogels, it may be observed that, irrespective of the reduction protocol used (and with the exception of the poorly reduced 10PtRuCX18-F sample), the catalysts supported on the oxidised xerogel, CX18, are twice as active as those supported on CX. This is a very interesting result, which might be explained by the surface chemical state of the two metals. Therefore, XPS analyses were carried out in order to investigate this effect.

3.4. XPS analyses

Samples 10PtCX-S, 10PtCX18-S, 10PtRuCX-S and 10PtRuCX18-S were analysed by XPS in order to evaluate the effect of the support on the nature and relative surface concentrations of the metals. The Pt 4f and Ru 3p spectra of the bimetallic samples were analysed and the deconvolution results of the Pt $4f_{7/2}$ and Ru $3p_{3/2}$ regions are shown in Table 6. All samples exhibit two components for the Pt $4f_{7/2}$ region, one attributed to metallic Pt at around 71.1 eV, and the other to Pt oxide (Pt^{2+}) at around 72.1 eV. In this region, there are no significant differences among the four samples, metallic Pt being the predominant species. Nevertheless, sample 10PtRuCX-S shows a slight increase, and sample 10PtRuCX18-S a slight decrease of Pt oxide. The Ru $3p_{3/2}$ region was selected for detailed analysis, because the Ru 3d and C 1s are partially overlapped, making difficult the quantitative analysis of the respective oxidation states. The main peak was deconvoluted into three peaks centered at around 462.0 eV, 463.7 eV and 466.6 eV, which are ascribed to metallic Ru, Ru oxide (Ru^{4+}) and hydrated Ru oxide ($RuO_2 \cdot xH_2O$), respectively [21,24]. There is a significant difference between the two bimetallic samples. In the case of the oxidised support (10PtRuCX18-S) there is a higher percentage of metallic Ru and almost no hydrated Ru^{4+} species. Another important difference between the bimetallic samples is that the surface Pt/Ru atomic ratio is 1.0 for sample 10PtRuCX18-S, as expected, but only 0.32 for sample 10PtRuCX-S. According to Aricò et al. [2], the optimum Pt:Ru atomic ratio is 1:1, which, together with the higher contents of metallic Ru on the surface of 10PtRuCX18-S, might explain the higher activities of the catalysts supported on the oxidised xerogel. This result is in agreement with a very recent report [25], where a remarkable increase in activity was observed for a Pt–Ru catalyst supported on

Table 6
XPS results

Sample	Pt/Ru atomic ratio	Pt $4f_{7/2}$			Ru $3p_{3/2}$		
		Species	B.E.(eV)	%	Species	B.E.(eV)	%
10PtCXS	–	Pt(0)	71.1	65	–	–	–
		Pt(II)	72.1	35	–	–	–
10PtCX18S	–	Pt(0)	71.0	66	–	–	–
		Pt(II)	72.0	34	–	–	–
10PtRuCXS	0.32	Pt(0)	72.6	63	Ru(0)	462.3	27
		Pt(II)	73.6	37	Ru(IV)	463.5	54
					Ru(IV)-hydrated	466.5	19
10PtRuCX18S	1.0	Pt(0)	71.2	69	Ru(0)	461.8	49
		Pt(II)	72.1	31	Ru(IV)	463.9	48
					Ru(IV)-hydrated	466.6	3

a H_2O_2-functionalized carbon black. The authors explained this effect by the type and surface density of the oxygen-containing groups developed after the H_2O_2 treatment, and a similar reasoning might be applicable in the present situation. It is quite interesting that the catalyst supported on the oxidised xerogel is less oxidised (cf. Table 6) than that supported on CX. Higher oxidation states of Ru and Pt in the 10PtRuCX-S catalyst lead to a lower activity for methanol electro-oxidation.

4. Conclusions

It was found that, in general, the reduction of the catalyst with sodium borohydride leads to higher dispersion and more homogeneous distribution of the metal particles on the supports. In addition, the xerogel-supported catalysts showed higher activity than those supported on carbon nanotubes. A remarkable increase in the activity for methanol electro-oxidation was observed when the Pt–Ru catalysts were supported on the oxidised xerogel. This effect was not so notorious in the case of the Pt catalysts. XPS analyses showed that the oxidation state of Pt in the monometallic catalysts did not change significantly; however, in the case of the Pt–Ru alloy catalysts, the oxidised support helped to maintain the metals in the metallic state, as required for the electro-oxidation of methanol.

Acknowledgements

This work was supported by ''Fundação para a Ciência e a Tecnologia'', under programme POCTI/FEDER (POCTI 1181), and by the Indo-Portuguese Cooperation Programme in Science and Technology, GRICES/DST.

References

[1] Hogarth MP, Ralph TR. Catalysis for low temperature fuel cells. Platinum Metals Rev 2002;46:146–64.
[2] Aricò AS, Srinivasan S, Antonucci V. DMFCs: from fundamental aspects to technology development. Fuel Cells 2001;1:133–61.
[3] Bessel CA, Laubernds K, Rodriguez NM, Baker RTK. Graphite nanofibers as an electrode for fuel cell applications. J Phys Chem B 2001;105:1115–8.
[4] Steigerwalt ES, Deluga GA, Lukehart CM. Pt–Ru/carbon fiber nanocomposites: synthesis, characterization, and performance as anode catalysts of direct methanol fuel cells. A search for exceptional performance. J Phys Chem B 2002;106:760–6.
[5] Li W, Liang C, Qiu J, Zhou W, Han H, Wei Z, et al. Carbon nanotubes as support for cathode catalyst of a direct methanol fuel cell. Carbon 2002;40:791–4.
[6] Carmo M, Paganin VA, Rosolen JM, Gonzalez ER. Alternative supports for the preparation of catalysts for low-temperature fuel cells: the use of carbon nanotubes. J Power Sources 2005;142:169–76.
[7] Li W, Liang C, Zhou W, Qiu J, Li H, Sun G, et al. Homogeneous and controllable Pt particles deposited on multi-wall carbon nanotubes as cathode catalyst for direct methanol fuel cells. Carbon 2004;42:436–9.
[8] Frackowiak E, Lota G, Cacciaguerra T, Béguin F. Carbon nanotubes with Pt–Ru catalysts for methanol fuel cell. Electroch Commun 2006;8:129–32.
[9] Hyeon T, Han S, Sung YE, Park KW, Kim YW. High performance direct methanol fuel cell electrodes using solid-phase-synthesized carbon nanocoils. Angew Chem Int Ed 2003;42:4352–6.
[10] Che G, Lakshmi BB, Martin CR, Fisher ER. Metal-nanocluster-filled carbon nanotubes: catalytic properties and possible applications in electrochemical energy storage and production. Langmuir 1999;15:750–8.
[11] Chai GS, Yoon SB, Yu JS, Choi JH, Sung YE. Ordered porous carbons with tunable pore sizes as catalyst supports in direct methanol fuel cell. J Phys Chem B 2004;108:7074–9.
[12] Rao V, Simonov PA, Savinova ER, Plaskin GV, Cherepanova SV, Kryukova GN, et al. The influence of carbon support porosity on the activity of PtRu/Sibunit anode catalysts for methanol oxidation. J Power Sources 2005;145:178–87.
[13] Moreno-Castilla C, Maldonado-Hódar FJ. Carbon aerogels for catalysis applications: an overview. Carbon 2005;43:455–65.
[14] Job N, Théry A, Pirard R, Marien J, Kocon L, Rouzaud JN, et al. Carbon aerogels, cryogels and xerogels: influence of the drying method on the textural properties of porous carbon materials. Carbon 2005;43:2481–94.
[15] Gomes HT, Samant PV, Serp P, Kalck P, Figueiredo JL, Faria JL. Carbon nanotubes and xerogels as supports of well dispersed Pt catalysts for environmental applications. Appl Catal B: Environmental 2004;54:175–82.
[16] Samant PV, Rangel CM, Romero MH, Fernandes JB, Figueiredo JL. Carbon supports for methanol oxidation catalyst. J Power Sources 2005;151:79–84.
[17] Corrias M, Caussat B, Ayral A, Durand J, Kihn Y, Kalck P, et al. Carbon nanotubes produced by fluidized bed catalytic CVD: first approach of the process. Chem Eng Sci 2003;58:4475–82.
[18] Pekala RW. Organic aerogels from the polycondensation of resorcinol with formaldehyde. J Mater Sci 1989;24:3221–7.

[19] Samant PV, Gonçalves F, Freitas MMA, Pereira MFR, Figueiredo JL. Surface activation of a polymer based carbon. Carbon 2004;42:1321–5.

[20] Figueiredo JL, Pereira MFR, Freitas MMA, Órfão JJM. Modification of the surface chemistry of activated carbons. Carbon 1999;37:1379–89.

[21] Aricò AS, Vaglio V, Di Blasi A, Modica E, Antonucci PL, Antonucci V. Analysis of the high-temperature methanol oxidation behaviour at carbon-supported Pt–Ru catalysts. J Electroanal Chem 2003;557:167–76.

[22] Sarma LS, Lin TD, Tsai Y-W, Chen JM, Wang BJ. Carbon-supported Pt-Ru catalysts prepared by the Nafion stabilized alcohol reduction method for application in direct methanol fuel cells. J Power Sources 2005;139:44–54.

[23] Rojas S, García-García FJ, Jaras S, Martínez-Huerta MV, Fierro JLG, Boutonnet M. Preparation of carbon supported Pt and PtRu nanoparticles from microemulsion electrocatalysts for fuel cell applications. Appl Catal A: General 2005;285:24–35.

[24] Raman RK, Shukla AK, Gayen A, Hedge MS, Priolkar KR, Sarode PR, et al. Tailoring a Pt–Ru catalyst for enhanced methanol electro-oxidation. J Power Sources 2006;157:45–55.

[25] Gómez de la Fuente JL, Martínez-Huerta MV, Rojas S, Terreros P, Fierro JLG, Peña MA. Enhanced methanol electrooxidation activity of PtRu nanoparticles supported on H_2O_2-functionalized carbon black. Carbon 2005;43:3002–5.